International Journal of Recent Technology and Engineering (IJRTE)
ISSN: 2277-3878 (Online), Volume-9 Issue-6, March 2021

Effect of Aging and Deformation Treatments on Mechanical Properties of Aluminum AA-6063

Víctor Alcántara Alza

Abstract*: *How the parameters of artificial aging heat treatments, in AA 6063 aluminum samples, previously solubilized and deformed in cold, influence on the mechanical properties of hardness and traction was investigated. The experiments followed the sequence: First, the solubilization treatment was carried out for 2h using prismatic specimens of 10mm thickness; then the samples were cold deformed with area reductions: 30% -60% -80%. Finally, the aging treatment was carried out on all samples, using temperatures: 150-250-350-450 °C, and holding times: 1-10-30-60-90-120 min. After aging the samples were machined according to the standards. The hardness was measured on the Vickers scale (HV) and the tensile tests followed the ASTM E 8M-95ª standard. Microscopy was performed at the optical and Electronic SEM level, complemented with an EDS analysis. It was found that the highest hardness values occur at 150 °C. The yield point YS increases as decreasing aging temperature, and decreases whith increasing deformation degree. The mechanical strength UTS increases as decreasing temperature and increasing whith deformation degree. Regarding the mechanical properties of traction, the optimal condition is found for the samples deformed at 80% and aged at 250 °C, presenting a (UTS) of 193 MPa, and 15% elongation. The samples with 80% reduction, aged at 450 °C for 120 min are those with the best recrystallization index. It would take a time greater than 120 min for the grains to thicken and the precipitates completely disappear to reach complete recrystallization. EDS analysis indicates the presence of Mg2Si precipitates and the β phase.

Keywords*: *Aging, cold deformation, aluminum 6063, recrystallization

I. INTRODUCTION

Aluminum is one of the main materials used in modern industry, due to the combination of some properties that make it very useful in various applications, such as its low density and high resistance to corrosion, good conductor of electricity, easily machined and relatively inexpensive. For these reasons, it is the metal most used in modern industry after steel **[1].** Its great applicability is found, in the maritime, land and aeronautical transport industry; and they have contributed greatly to the improvements of vehicles and machines, providing structural strength and considerable weight reduction, as well as resistance to corrosion. In the automotive industry there is a growing demand for aluminum alloys; since by reducing the weight of the vehicles, there is less fuel consumption, and control of the emission of gases. These advantages have attracted great attention in automotive applications due to its excellent molding capacity, corrosion resistance and especially its high weight / resistance ratio **[2], [3].**

Unlike steels, heat treatments in aluminum alloys are mainly restricted to the operation destined to increase the mechanical resistance (UTS) and hardness by means of the aging treatment or hardening by precipitation; which makes this treatment an important hardening method, which is used to increase the strength and hardness of most aluminum alloys **[4], [5], [6].**

Aluminum alloys are very diverse, due to the variety of alloying elements, mainly Copper, Magnesium, Manganese, Silicon and Zinc, which influence on the UTS in one way or another. The ANSI assigns each aluminum alloy a four-digit number, of which the first refers to the main alloying element. Based on these, there are the following alloy groups: 1xxx series unalloyed aluminum, 2xxx series with copper as the main alloying element, 3xxx series with manganese, 4xxx series with silicon, 5xxx series with magnesium, 6xxx series with magnesium and silicon, 7xxx series with zinc and in some cases magnesium, 8xxx series for other elements, although recently the 9xxx lithium alloys have been added to these series for unusual alloys **[4].** All these alloys are hardened by heat treatment or by deformation.

Of all the aluminum alloys, the 6xxx series are the most used for structural applications in various industrial sectors, due to their low density (one third of steel) with good mechanical properties **[7], [8], [9], [10].**

According to Troeger **[11],** 6xxx alloys have other benefits, such as good formability, weldability, resistance to corrosion. He claims that such alloys can be used in a variety of applications, including aircraft fuselage skins and automobile body panels, and are cheaper than the 2xxx and 7xxx series, after appropriate heat treatments. The main components of the 6xxx series aluminum alloy are Mg and Si, and these 6xxx alloys owe their strength to the Mg_2Si phase, (intermetallic compound) that is formed during the precipitation hardening treatment. This hardening occurs through solution treatment and artificial aging, which provides growth control and a composition consisting of a matrix rich in aluminum **[11], [12]**. However, if there is an excessive growth of these precipitates through treatments at high temperatures or very long times, the movement of dislocations is facilitated, it is brought about by the softening of the alloy. The treatment that produces this result is called over-aging. Silicon helps to generate high dislocation densities, but at the same time influences the reduction of the ductility of the material.

Manuscript received on March 13, 2021.
Revised Manuscript received on March 18, 2021.
Manuscript published on March 30, 2021.

Víctor Alcántara Alza, Department of Mechanics and Energy, National University of Trujillo, Perú. Email: victoralc_unt@hotmail.com

On the other hand, it has been shown how the Mg / Si ratio controls the hardness of the material so that an excess of Mg with respect to silicon (Mg / Si> 1.7) helps to maintain its constant value after aging **[13].**

Volume fraction of Mg2Si precipitate, depends on the level of Mg within the alloy, but the Si content is also important. Hirth et al.

[14] concluded that the increase of Si in the alloys type 6xxx increases the UTS with the treatments T4 and T6. [Natural and artificial treatment of aging and solubilization respectively].

Much research has been carried out regarding the 6xxx series aluminum alloys, and especially the AA-6063 alloy, of which the following should be highlighted:

E. Tan and B. Ögel **[15]** studied the influence of heat treatments on the mechanical properties of AA 6066 aluminum alloy under strain conditions. The objective was to produce high-strength, fine-grained 6xxx aluminum alloys by adjusting the process parameters: deformation, solution, and aging. The ideal solution temperature was found to be 530 ° C. Below 530 ° C, there is a tendency to increase hardness with increasing soaking time, while the trend is reversed for higher temperatures. When carrying out the aging tests, the maximum hardness values of 175 °C were found for 8 h. The micostructure, showed the precipitated phase Mg_2Si. With samples deformed up to 10% before the dissolution process, the lowest YS is obtained. As the amount of strain increased, the recrystallized grain size became smaller, increasing the UTS and hardness of the samples

N. Anjabin and A. K. Taheri, **[16],** studied the effect of aging treatment on the mechanical properties of AA-6082 alloy, using an analytical model with optimized constants. It was found; that for a constant aging time and low temperatures YS increases and the elongation decreases. On the contrary, under over-aging conditions YS decreases and elongation increases. The results predicted by the model showed good agreement with the experimental data.

B. Milkereit et al, **[17]** investigated the precipitation behavior as a function of temperature and time of Aluminum alloys: 6060, 6063, 6005A and 6082 at different cooling rates after solution annealing. The CCT diagrams of each of the alloys were recorded. It was found that an appropriate range of cooling rates, all alloys show a similar precipitation behavior. High-temperature reactions produce the precipitation of the Mg_2Si equilibrium phase, and low-temperature reactions produce the precipitation of the β 'and β' phases. They concluded that maximum hardness values should always be found in materials that cool faster than the alloy-specific critical cooling rate, which increases with increasing alloy content.

M. Das et al. **[18]** studied the microstructure characteristics and mechanical properties of alloy 6063 processed with severe plastic deformation by torsion, after a solution treatment. No precipitates were observed in the dissolution condition, but after deformation very fine precipitates of Mg2Si were observed varying between 10-20 nm in size. The YS and UTS mechanical properties increased with the level of deformation.

J. Lan, et al, **[19]** established that in aluminum alloys, the introduction of cold deformation before aging is an important hardening method. They carried out an experiment with the 2A14 alloy, using 4 prediction models that were subjected to experimental testing. The precipitated phases θ, θ ', θ´´ were observed in the aging process after cold deformation. The greater the cold deformation, the more obvious its effect on the precipitation reaction. For the four models of hardening mechanisms, the predicted YS values of the 2A14 aluminum alloy during the aging process coincided with the experimental value, while the cold deformations were less than or equal to 6%.

The objective of this work is to determine the effect produced by the variation of the aging treatment parameters after a solubilization treatment and percentage of cold deformation, on the mechanical properties of hardness, YS, UTS, elongation and microstructure characteristics in aluminum alloys AA 6063

II. MATERIALS AND METHODS

2.1. Study Material

The AA-6063 alloy is an aluminum alloy with magnesium and silicon as basic elements. It has good mechanical properties and is heat treatable by precipitation and is also weldable. It is the most common alloy used for aluminum extrusion. It allows the forming of complex shapes with very smooth surfaces, suitable for anodizing and is therefore popular for visible industrial and architectural applications such as window frames, door frames, ceilings and signage frames. Its chemical composition can be seen in table 1.

Table 1. Chemical composition of aluminum: 6063 (w%)

%	Si	Fe	Cu	Mn	Mg	Cr	Zn	Ti	Otros	Al
Min	0.20				0.45					
Max	0.60	0.35	0.10	0.10	0.90	0.10	0.10	0.10	0.15	Resto

The material was purchased in the delivery condition, under annealing treatment (T0 temper) with a Vickers hardness of 25 HV. The supply microstructure can be seen in Fig. 1. and the CCT continuous cooling diagram in Figure 3.

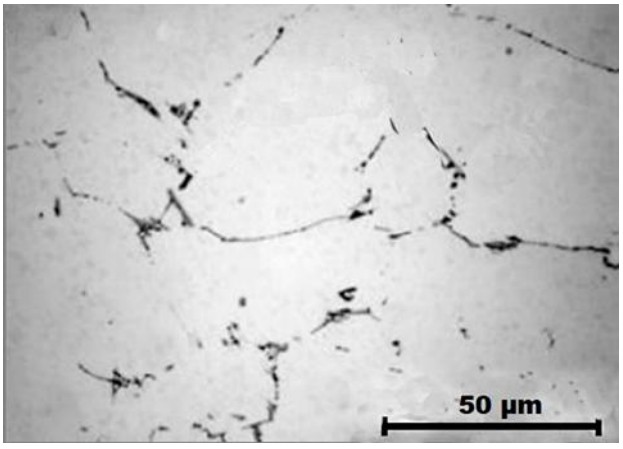

Figure 1. Microstructure of the material in the delivery state with annealing treatment (T0). A coarse-grained structure is observed with precipitates at the grain edges. Sample Hardness: 25 HV.

2.2. Treatments and Parameters Sequence.

Todas las muestras fueron sometidas a un proceso de tratamientos de envejecido y deformación (Tratamiento termo-mecánico), siguiendo la siguiente secuencia:

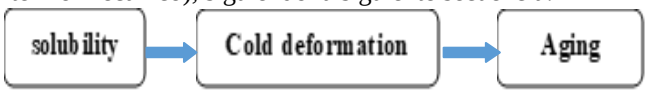

The sequence of thermal and mechanical deformation treatments (Thermomechanical) that were carried out can be seen in figure 2.

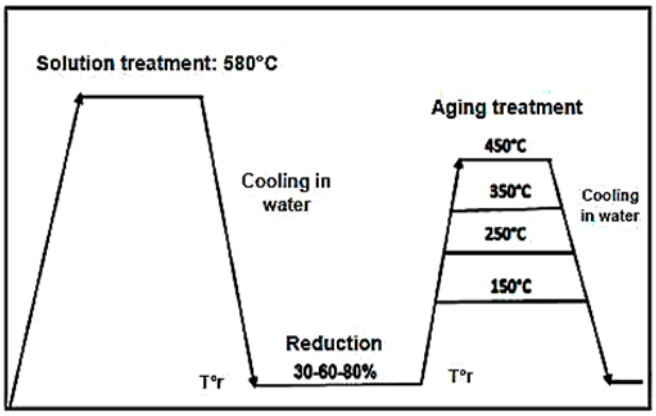

Figure 2. Scheme of the sequence of heat and mechanical deformation treatments used. (T°r = Room temperature)

The solubility treatment was carried out, at temperature of 580°C, for 1h, followed by cooling in water. This temperature and time was selected, following commercial standards and taking into account the CCT diagram of Figure 3. The treatment was carried out in a THERMOLYNE digital electric oven. After the solubilization treatment, the samples were cold deformed to obtain the respective area reduction according to the reduction percentage. For reduce the area of the solubilized samples, a small laminator was used with cylinders of 2" (50.4 mm) mm in diameter x 220 mm in length. Three area reductions were made to all samples after solubilization: **30-60-80%** with respect to their original thickness of 10 mm. These deformations were carried out at room temperature.

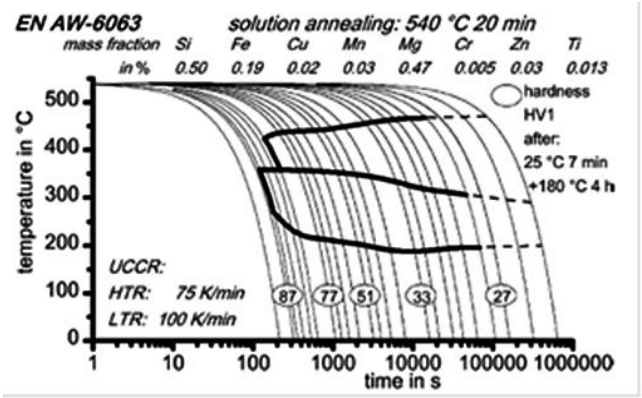

Figure 3. AA 6063 Aluminum CCT Diagram [22]

The aging treatment (precipitation) was T6 type. It was carried out in the same Thermolyne digital oven using the temperatures**: 150 °C, 250 °C; 350 °C; 450 °C** and holding times**: 1-10- 30- 60- 90- 120** (min). The times were sustained for each temperature level. After removing each sample from the oven, they were immediately cooled in water.

2.3. Experimental Procedure.

2.3.1. Samples

All the specimens were made from standard plates 12.50 mm thick x 1.06 m wide x 3.00 m long. Prismatic bars 100mm x 100mm x 10mm (thickness) were cut from these plates. The samples were ready for the solubilization, deformation and aging treatments. After being solubilized, the samples were deformed in a small laminator until reaching thicknesses of 7mm, 4mm and 2mm, which correspond to the percentages of deformation: 30-60-80%. They were then machined according to the standards of the hardness and traction tests; then they underwent the aging treatment before making the respective tests.

2.3.2. Hardness Test

The hardness test was performed on the Vickers HV-5/10/30/50, Digital Durometer used for non-ferrous materials.

From 100mm x 100mm x 10mm (thickness) aged samples, parallelepipeds of the following dimensions: 10x20x30mm. were made:

The test was carried out according to the ASTM E384 standard, using a load of 120Kgf (1176.8 N) with an indection time in the range: 10-15 s.

To carry out this test, the specimens previously had to be ground and polished on their surface to guarantee the parallelism between them, and the measurement is correct. The grinding was carried out on a COZZI flat grinding machine and sandpaper: 400, 800 and alumina cloth were used for polishing. After polishing, the specimens were tested and indented three times (3) for each measurement, averaging the results on the HV scale.

2.3.3. Tensile test.

The tensile tests were carried out on the IMSTRON UNIVERSAL 8801 machine with a 10 Ton capacity. The spcimens that were used followed the ASTM E8M-95 standard. The spcimens were machined under the established standard, whose measurements scheme is shown in Figure 4.

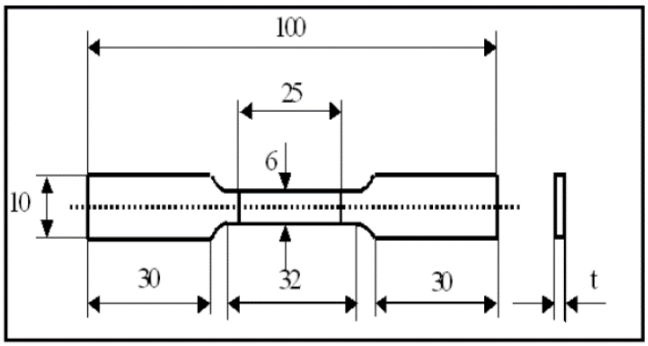

Figure 4. Plane for making tensile test specimens according to ASTM E8M-95 standard.

The "t" values shown in figure 4 were: 7-4-3 mm, which represent the degrees of deformation: 30-60-80% respectively. Figure 5 shows some representative specimens (reduction to 30%), after being aged and tested by traction. It can be seen that in all cases the break has occurred within the area of the calibrated length and shows a brittle break.

No ductile failure was observed in all samples. This indicates the high degree of hardening and embrittlement caused by the precipitation treatment and artificial aging.

2.3.4. Microscopy Test

The microscopy test was done at the optical level using the Zeiss 1000X Microscope,

and also the electronic level using the JEOL-JSM-5600 SEM (scanning electron microscope). The same equipment allows to carry out the Energy Spectroscopy test. Dispersed (EDS). Finally, the samples were encapsulated and polished and then they were attacked using as a reagent a solution composed of: (99.5 ml of water + 0.5 ml of hydrofluoric acid).

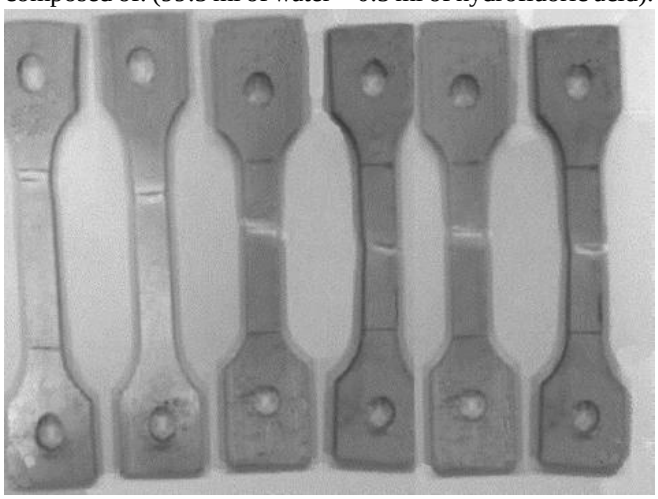

Figure 5. Tensile specimens tested for 30% deformed and aged samples. A brittle fracture is observed within the length tested.

III. RESULTS AND DISCUSSION

3.1 Hardness.

The hardness results for various deformation and aging conditions can be seen in tables 2, 3 and 4 and their corresponding trend graphs in figures: 6 (a), 6 (b) and 6 (c) respectively.

For samples deformed to 30%

Fig. 6a shows the following: For an aging temperature of 150 ° C; in the first minute the hardness rises from 25 HV to 70.2 HV. Then, in the next 20 min, increases until reaches to 86HV, and then progressively and slowly increases up to 92HV. For samples aged at 250 ° C; It is observed that in the first 10 minutes the hardness rises to 70 HV, and then decreases in the next 20 min until reaches to ~ 63HV, then it remains almost constant until the end of the interval. For samples aged at 350 °C, it is observed that in the first min the hardness rises to 69 HV, and then decreases to 52 HV when it reaches to 10 min, then it increases until ~65 HV upon reaching to 60 min, keeping that value almost constant until the end of the interval. For samples aged at 450 ° C; the trend is the same as for the previous case. The results show that the solubilized treatment and artificial aging notably increase the hardness from the beginning of the treatment. In the first minute increases from 25 HV for the supply state T(0) to values ~ 70 HV. In other words, the hardness almost triples in value in the first minute, showing the strong influence of cold water tempering. On the other hand, the lowest temperature (150 ° C) is the one that increases the hardness the most. The general trend observed is that the lower the temperature, the more the hardness increases, and with respect to the aging time, it can be reported that from 60 min to 120 min the hardness is almost not affected.

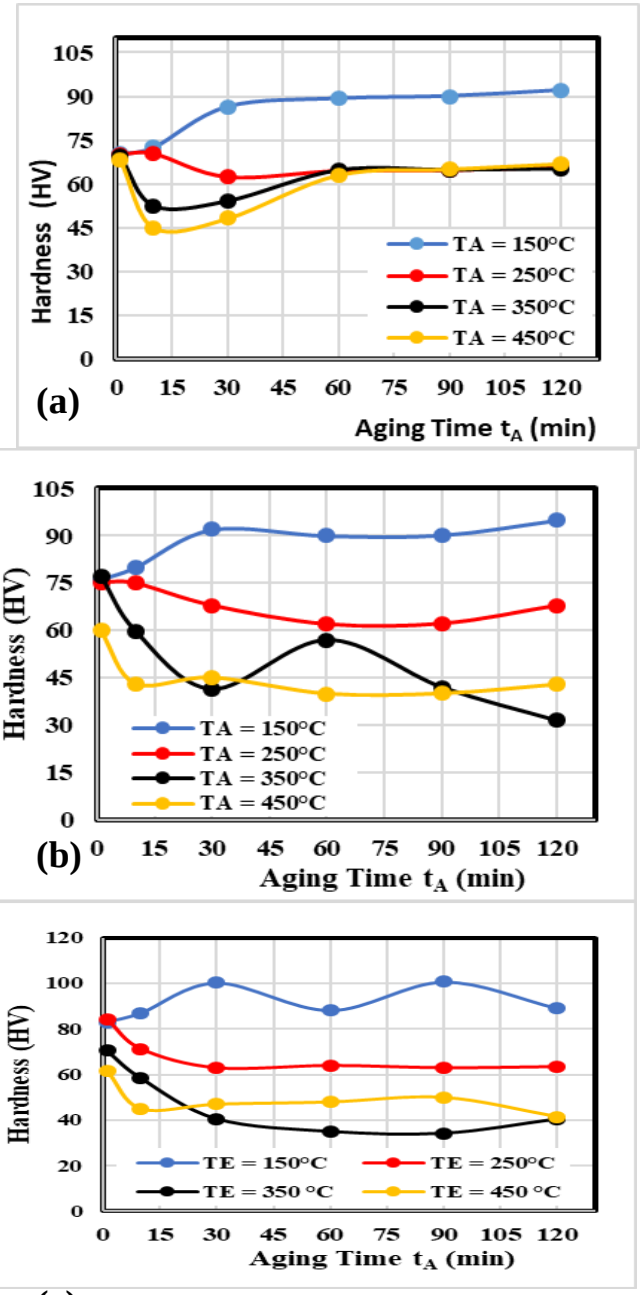

Figure 6. Graphs of variation of the hardness with the aging temperature (TE) and aging time (t_A), for AA6063 aluminum samples, according to the deformation percentage: a) 30%; b) 60%; c) 80%.

For samples deformed to 60%

In Fig. 6b) the graph of the deformed and aged samples with 60% reduction is shown. In the first minute the hardness is almost the same (~75HV), for the first three aging temperatures, with the exception of 450 ° C which presents a value of 60 HV. As in the previous case, it can be observed that: The hardness decreases as the aging temperature increases, and varies with the holding time. Thus we have:

For the temperature of 150 °C, the hardness increases with

Table 2. Hardness results for different aging times and temperatures with 30% deformation.

t_A (min)	HARDNES (HV)- 30% deformatión			
	T_E = 150°C	T_E = 250°C	T_E = 350°C	T_E= 450°C
1	70,2	70,0	69,3	68,0
10	72,5	70,2	52,3	45,0
30	86,4	62,3	54,0	48,2
60	89,2	64,4	64,7	63,0
90	90,0	64,6	64,8	65,0
120	92,0	65,8	65,2	66,8

Table 3. Hardness results for different aging times and temperatures with 60% deformation

t_A (min)	HARDNESS (HV) – 60% deformation			
	T_E = 150°C	T_E = 250°C	T_E = 350°C	T_E= 450°C
1	76,0	75,3	77,2	60,0
10	79,8	75,0	59,8	43,2
30	92,0	68,0	41,5	45,2
60	90,0	62,1	57,0	40,0
90	90,2	62,3	42,0	40,1
120	95,0	68,0	31,5	43,0

Table 4. Hardness results for different aging times and temperatures with 80% deformation

t_A (min)	HARDNESS (HV) – 80% deformation			
	T_E = 150°C	T_E = 250°C	T_E = 350°C	T_E= 450°C
1	83,0	84,2	70,5	61,8
10	87,0	71,2	58,4	45,0
30	100,3	63,0	40,5	47,0
60	88,1	64,0	35,0	48,0
90	100,7	63,0	34,2	50,0
120	89,0	63,5	40,5	41,5

holding time. For the temperature of 250 °C the hardness decreases with the aging time with an almost constant slope. For the temperature of 350 °C the hardness decreases with the aging time, but in an oscillating way. For a temperature of 450 °C it decreases with the aging time, its values overlapping with the temperature of 350 °C in different time intervals.

For samples deformed to 80%

In Fig. 6c) the graph of the deformed samples with 80% reduction is shown. In this case it can also be observed that the hardness increases as the aging temperature decreases, with the exception of the 450 °C temperature, which presents higher hardness values than the 350 °C temperature. Regarding the holding time, we have:

For 150 °C, the hardness increases to 83 HV in the first minute and then shows oscillatory values as the holding time increases.

For 250 ° C, in the first minute it has the same value as the previous case and suffers a decrease until it reaches 30 minutes and then remains almost stable until 120 minutes. For 350 °C, the hardness in the first minute drops to 70.5 HV and then drops to 35 HV when reaching 60 min, and then increases to 40.5 HV until reaching 120 min.

When analyzing the three cases, it can be concluded that the highest hardness is found with the lowest temperature (150 ° C.) And time does not decrease the hardness. For the other temperatures, time in some cases decreases the hardness with an almost constant rate, and in others in an oscillating manner. For deformations of 60% and 80%, the hardness of samples aged at 450 ° C is greater than those aged at 350 ° C in certain sections, being more accentuated for deformation (80%) where it presents higher values in almost the entire interval.

3.1.1. Deformation effect on hardness [T°Aging = cte]

Figure 7 shows the graphs of hardness vs. aging temperature, varying the time and the deformation.

From the 4 graphs shown it can be inferred: That both the deformation percentage and the aging time are interdependent variables, which define the hardness of the treatment. They are not isolated variables; they are mutually interrelated.

For an aging temperature of 150 °C, it is observed that the higher the percentage of deformation, the higher the hardness in the entire time interval except for 60 min where the hardnesses are almost equal. For this temperature, the deformation is imposed on the increase in hardness; which is not the case with the other temperatures.

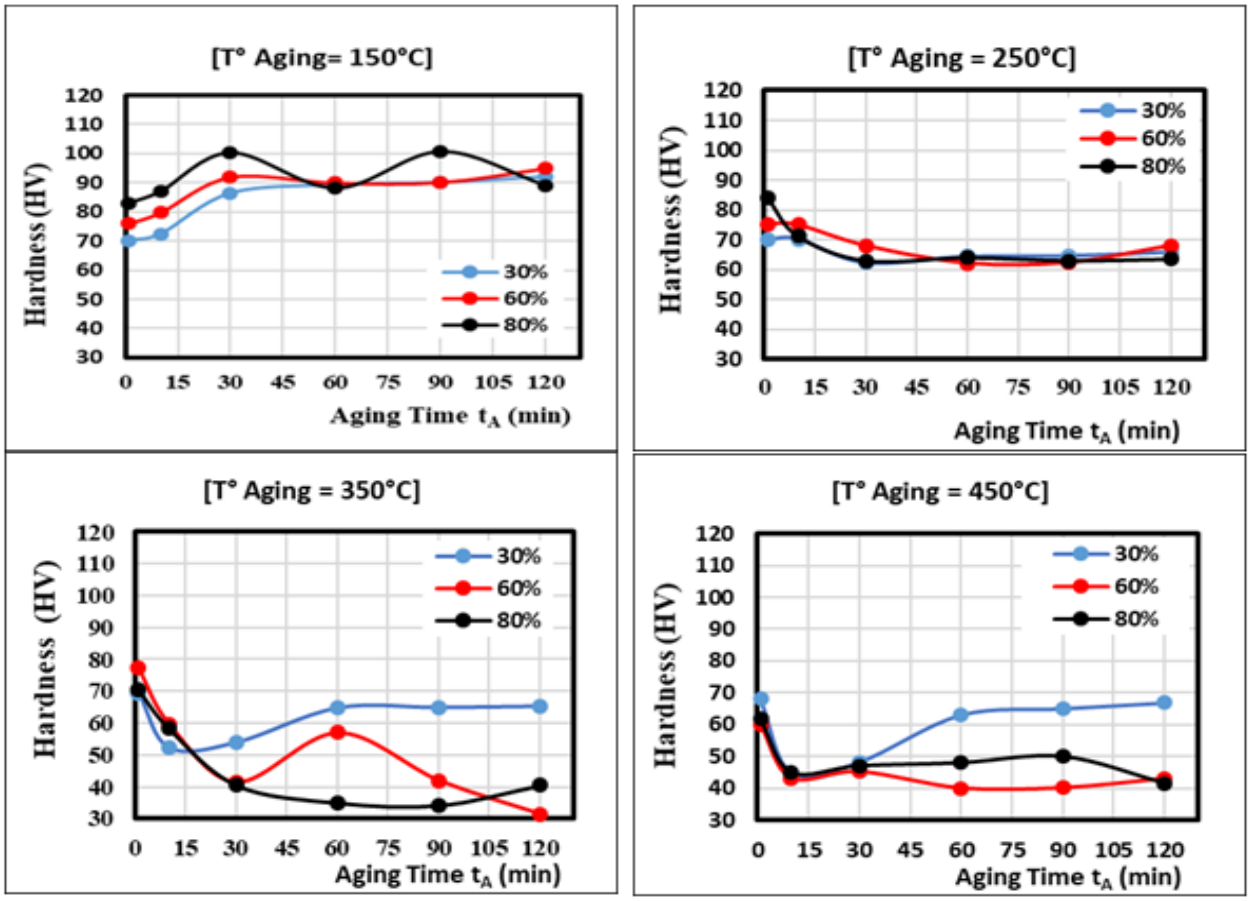

Figure 7. Graphs showing the effect of deformation on hardness as a function of aging time, keeping each test temperature constant.

For 250 °C, the relationship: greater deformation implies greater hardness is met only in the first 10 minutes, then the samples deformed to 60% present the highest hardness up to 45 minutes and from then on the three deformation curves present very close hardness. In other words: Time and deformation hardly affect hardness. For 350 ° C up to the first 10 minutes we have a trend similar to the previous case and thereafter the effect is reversed, in the sense that the lower deformation, the lower hardness. For 450 °C up to the first 30 minutes, for all three degrees of deformation, the hardness has almost the same value, and from there up to 120 min, the increase in hardness is established in the following order: 30%; 80% and 60% respectively. In this case, the least deformed samples have the highest hardness in this time interval. It can be inferred that: "The combined effect of the time - deformation variables in the artificial aging treatment, up to 120 min, tends to decrease the hardness of the samples". We can say nothing of longer aging times where diffusion phenomena can cause other types of precipitates that could increase hardness.

3.2. Tensile mechanical properties

The tensile tests were carried out on a selected group of samples:

1) For undeformed and solubilized samples.

2) For solubilized, deformed and aged samples at 150 °C and 250 °C, for a time holding of 2 h, considering the three reductions of areas (30%, 60% and 80%). Time variation has not been considered. The results can be seen in table 5 and in the graphs shown in the figures: From Fig. 8 to Fig. 11.

The legend presented in Table 5 only applies to solubilized and aged samples. It has also been considered to add the σ-ε graphs of the samples solubilized without deformation tempered in air and water.

Table 5. Tensile mechanical properties of selected samples

Type of sample	Mechanical properties		
	(YS) MPa	(UTS) MPa	Elongation (ε)
solubilized only			
Air Quenching	63	123	0.31
Wáter Quenching	85	137	0.32
Solubilized and aging			
Tipo 1	120	164	0.16
Tipo 2	110	183	0.11
Tipo 3	100	187	0.09
Tipo 4	110	152	0.21
Tipo 5	90	173	0.18
Tipo 6	80	193	0.15

Legend:
1) Def: 30%; Ta= 150°C; 2) Def: 60%; Ta= 150°C; 3) Def: 80%; Ta= 150°C; 4) Def: 30%; Ta= 250°C; 5) Def: 60%; Ta= 250°C; 6) Def: 80%; Ta= 250°C
t_A= 2h (In all cases)

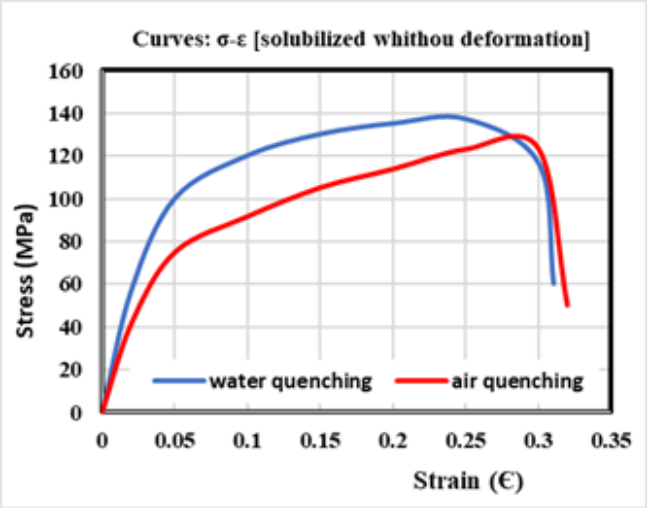

Figure 8. Tensile curves obtained for the samples solubilized at 580 ° C and tempered in air and water without deformation nor aging.

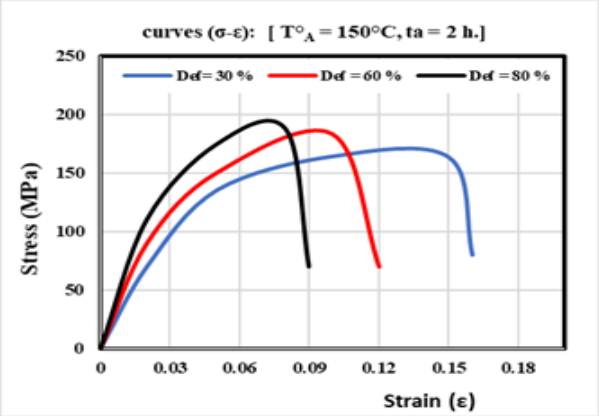

Figure. 9. Graphs of the tensile curves for samples solubilized at 580 ° C, deformed and aged at 150 ° C, 2 h.

Fig. 8 shows the tensile curves obtained for the undeformed samples, with solubilized without aging. The samples tempered in water show higher values of UTS (137 MPa), YS (85 MPa), with respect to the samples cooled in air, although both present almost similar elongation values (ε = 31%), demonstrating good ductility.

Fig. 9. shows the tensile curves obtained for samples aged at 150 ° C, 2 h. showing the effect of deformation. It is observed that a greater deformation causes a decrease in YS and an increase in UTS and a decrease in ductility ε

Fig. 10. show the graphs of the tensile curves obtained for the samples aged at 250 ° C; showing the same trend as for the previous case. There is not much variation in YS and UTS, but a significant increase in ductility. The increase in temperature has increased significantly the ductility ε, for all degrees of deformation.

Figs: 11 and 12 show the graphs: "Stress- Degree of deformation", parameterizing the two aging temperatures: 150 °C and 250 °C, without considering the aging time. It is observed that YS decreases with increasing deformation, while UTS increases as the degree of deformation increases.

If all the graphs of the tensile properties for these two temperatures are observed, the following conclusion can be drawn: The optimal condition is found for the sample deformed at 80% and aged at 250 ° C, presenting a tensile strength (UTS) of 193 MPa and 15% elongation, resulting in a good combination of strength and ductility. This condition corresponds to a hardness of 63.5 HV

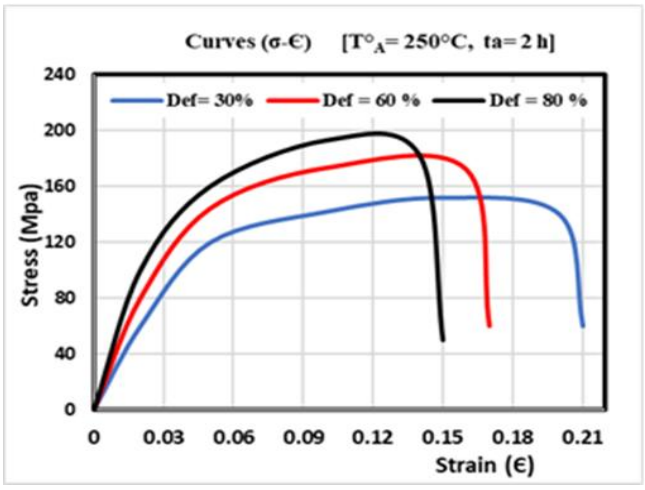

Figure10. Tensile curves for samples solubilized at 580 ° C, deformed and aged at 250 ° C, 2h.

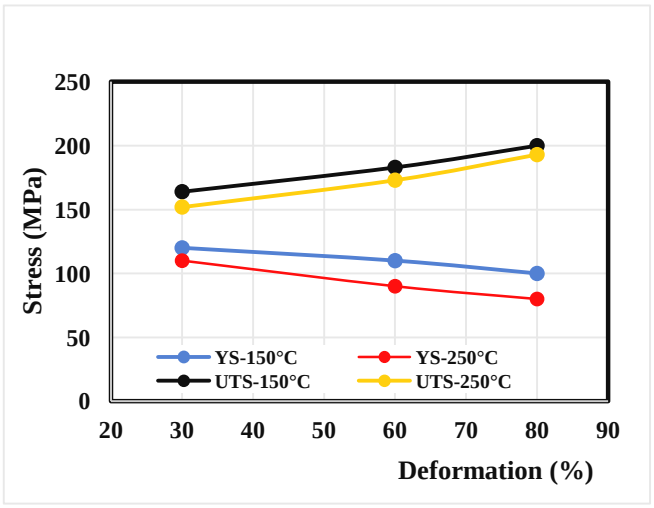

Figure 11. Graphs of (UTS) and (YS) as a function of the percentage (%) deformation. Solubilized T ° = 580 ° C; TE = (150 °C - 250 °C), 2 h.

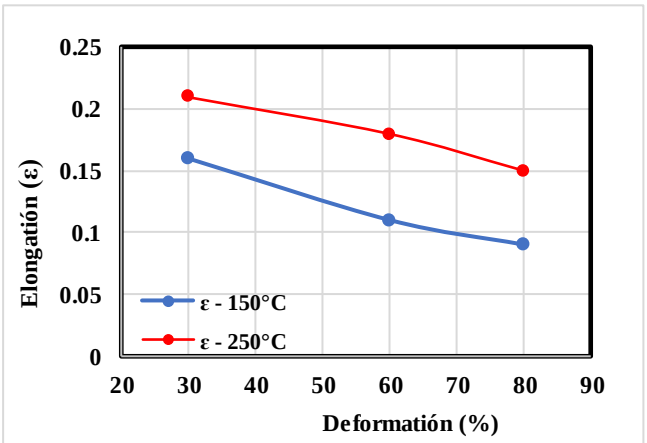

Figure 12. Graphs of elongation (ε) as a function of the percentage (%) deformation: for: T ° solubilized = 580 ° C; TE = (150 °C - 250 °C), 2 h.

3.3. Microstructure

The microstructure of the samples prior to aging (solubilized and tempered in water) is observed in the SEM photomicrograph of Figure 14. A coarse-grained matrix and scattered dark spots are observed, which can be non-metallic inclusions or precipitated phases, which are spherical or bar-shaped. EDS analysis indicates different compositions for these two points. The first indicates a large presence of aluminum with silicon and, being the Mg content high in the entire alloy, it indicates that it is the Mg2Si precipitate, according to **[11], [12].** The second indicates the presence of Cr and Cu; which makes it very likely that it is the β phase. In this 6063 aluminum type, both phases precipitate with aging.

The microstructure of the deformed and aged samples is observed in figure 13. Samples were taken for the three degrees of deformation with the four temperature levels, using two aging times: 90; 120 min. the details are indicated in the third column of the table containing the figures.

The material after the deformation processes, produces the extension of the grains that depend on the applied deformation. This deformation implies high energy retained in the material in the form of crystalline defects. When high values of deformation are achieved, an enormous density of defects is generated in the crystal line that are responsible for the increase in hardness. On the other hand, the aging time and temperature bring with it the recovery and recrystallization mechanisms that dampen the hardness induced by deformation, but at the same time, the temperature and time are responsible for a hardening by precipitation. All these factors being involved; therefore. it is justified that the hardness values increase in one circumstance and decrease in another. The analysis can be finished stating that, in any case, the hardness and mechanical resistance always increase considerably with respect to the supply condition, but in the aging they do not follow a stable trend.

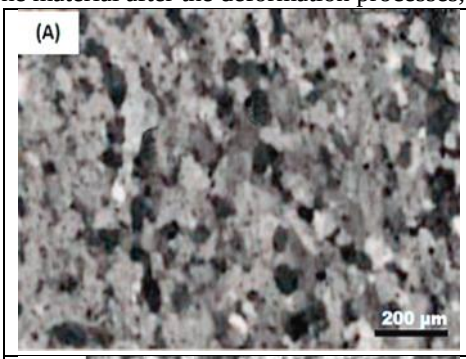	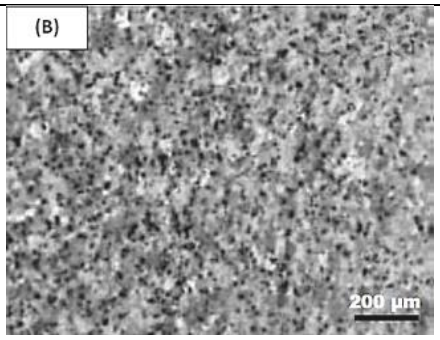	**REDUCTION: 30%** **AGED: 90 min** **(A) 150°C; (B) 250°C**
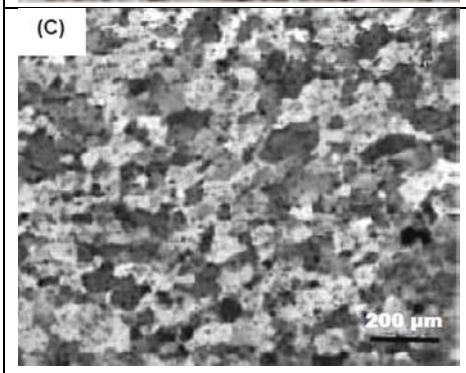	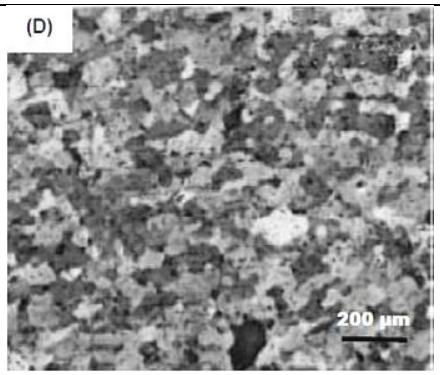	**REDUCTION: 30%** **AGED: 120 min** **(C) 150°C; (D) 250°C**
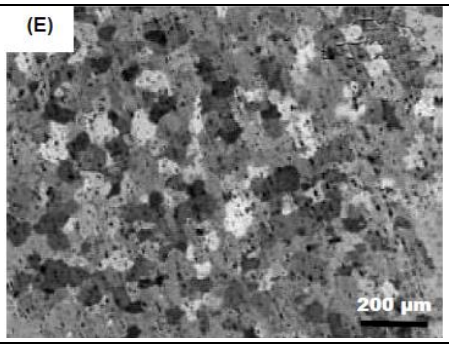	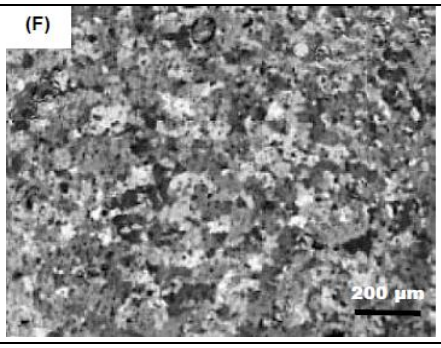	**REDUCTION: 60%** **AGED: 90 min** **(E) 350°C; (F) 450°C**

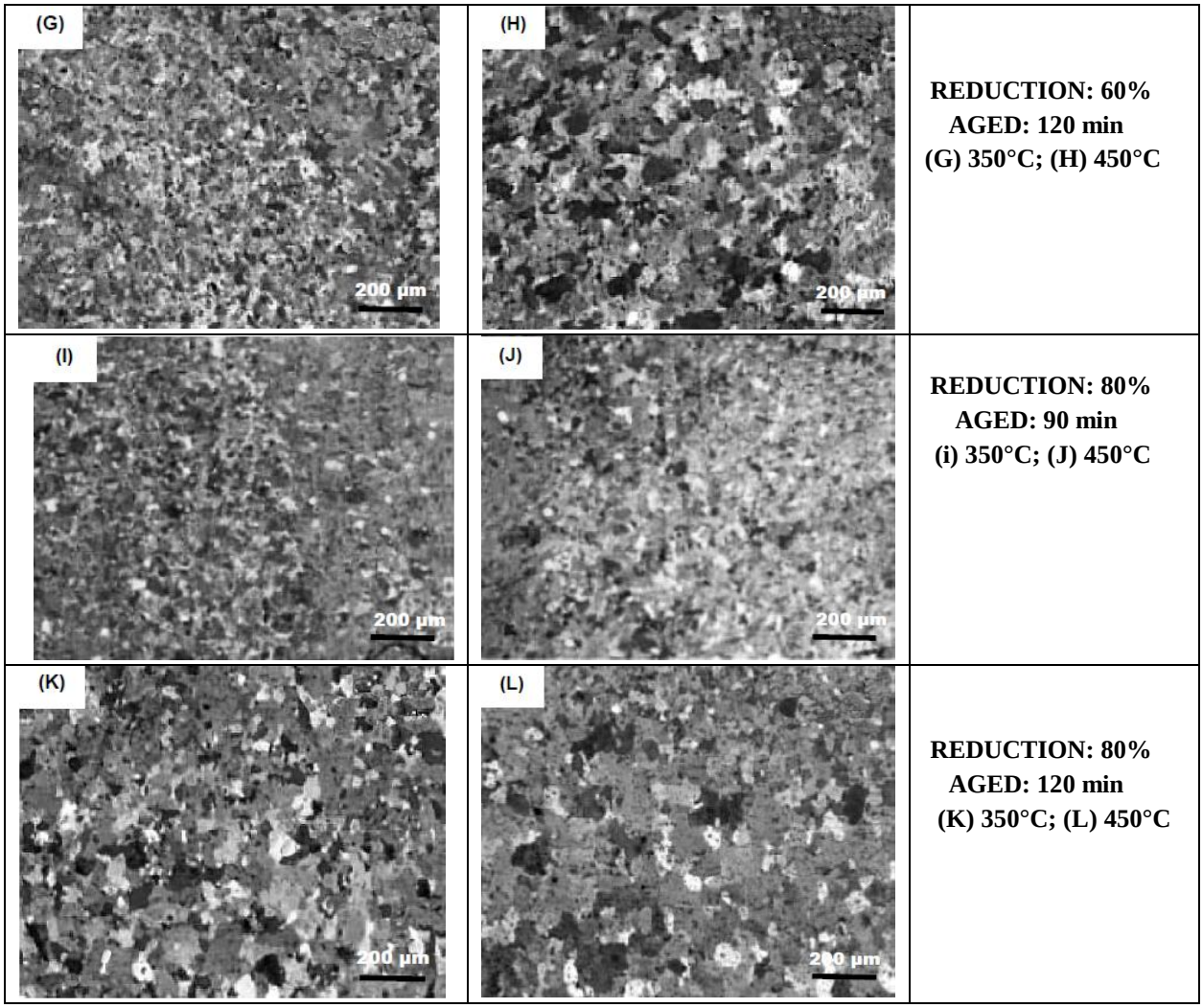

Figure 13. Optical micrographs of samples solubilized at 580 °C, deformed and then aged according to the attached table.

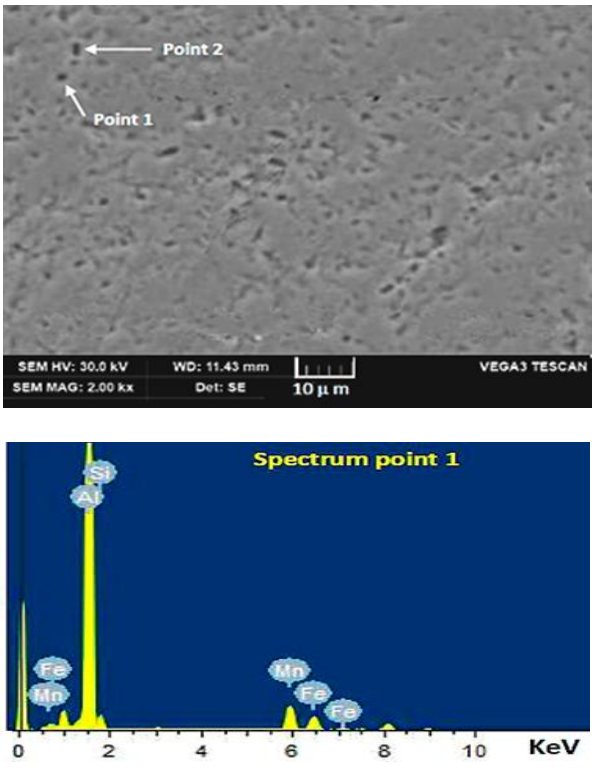

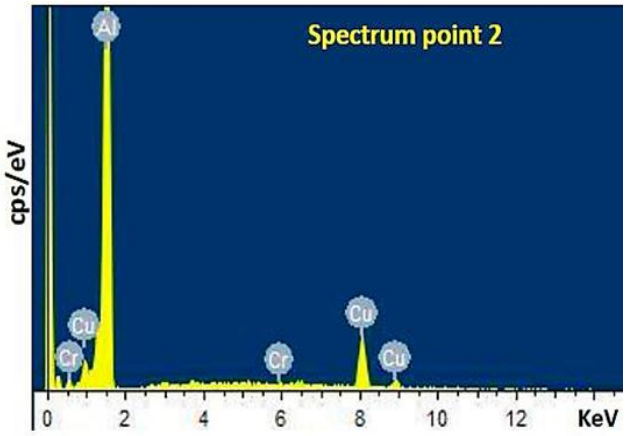

Figure 14. SEM photomicrograph of a 6063 aluminum sample, solubilized and cooled in water, before being deformed and aged. The EDS analysis is displayed for the indicated points.s.

The microstructures shown in figure 13 correspond to the samples aged after being solubilized and deformed. Samples aged at 150 °C; 90 min (Fig.13 a), still maintain elongated grains due to deformation.

Increasing the time to 120 min, (Fig. 13c) the recovery is observed without reaching recrystallization, since a large quantity of precipitates is observed.

With the same reduction, but aged at 250 °C, 90 min (Fig. 13b), the elongated grains disappear and intense precipitation is observed before reaching 120 min (Fig. 13d) where an almost recrystallized structure is shown. This phenomenon is repeated in a similar way for the other degrees of deformation. The samples with 80% reduction, aged at 450 °C for 120 min (Fig. 13L) are those with the best recrystallization index. It would take a time greater than 120 min for the grains to thicken and the precipitates completely disappear to reach complete recrystallization. Many research works show that for low temperatures, in any state of initial deformation, the aging process seems to be superimposed on the recovery-recrystallization **[20], [21].**

IV. CONCLUSION

From the study carried out on the effect of solubilization, deformation and aging treatments on hardness and tensile mechanical properties, can be extracted the following conclusions:

1. The three variables of the experiment: degree of deformation, aging time and temperature, are interdependent variables that define hardness and mechanical properties. They are not isolated research variables; they are mutually interrelated.

2. For all degrees of deformation, the artificial aging treatment produces a very pronounced increase in hardness in a short time (1 min), and then the hardness varies moderately, according to the treatment parameters: time, deformation and temperature.

3. The highest hardness values are found at the lowest temperature (150°C). The aging time in some cases increases the hardness, in others decreases, and others has an oscillating tendency.

4. An increase in deformation together with a low temperature and a longer aging time are the conditions that provide the maximum hardness values.

5. The yield point YS increases as decreasing aging temperature, and decreases whith increasing deformation degree. The mechanical strength UTS increases as decreasing temperature and increasing whith deformation degree. Elongation ε increases as increasing aging temperature and decreases with increasing deformation.

6. Regarding the mechanical properties of traction, the optimal condition is found for the samples deformed at 80% and aged at 250 ° C, presenting a (UTS) of 193 MPa, and 15% elongation; since is a good combination of high strength and good ductility in aluminum alloys.

7. The changes in the treatment parameters give rise to the presence of very fine particles that could be inclusions, intermetallic phase and/or light precipitates that are responsible for the irregularities in hardness and mechanical properties. As is the case with the Mg_2Si and β-phase particles that are common in this type of treatment.

REFERENCES

1. G. E. Téllez Fontecha, Respuesta al tratamiento térmico de envejecimiento de las aleaciones al-5mg y al-10mg modificadas con 2% de zinc, Proyecto de Grado para optar al título de Ingeniero Metalúrgico, Universidad industrial de Santander, Colombia, 2008.
2. A. Jambor, M. Beyer, New cars – New Material, Technical Report, Materials & Design, 18 (1997), pp. 203-209
3. Q. G. Wang, Microstructural Effects on the Tensile and Fracture Behaviour of aluminium Casting Alloys A356/357, Metallurgical and Materials Transactions A, Volume 34A (December 2003), pp. 2887-2899
4. F. Fracasso, Influence of quench rate on the hardness obtained after artificial ageing of an Al-Si-Mg alloy; Trabajo de tesis ejecutado en el área de materiales y manufactura del Instituto tecnológico de Jönköping, Suecia, 2010.
5. H. Kacar, E. Atik, C. Meric: Journal of Materials Processing Technology Vol. 142 (2003), p. 762.
6. N. Kamp, N. Gao, M.J. Starink, I. Sinclair: Int. Journal of Fatigue Vol. 29 (2007), p. 869.
7. D.J. Chakrabarti, D.E. Laughlin. Phase relations and precipitation in Al–Mg–Sialloys with Cu additions. Prog Mater Sci 2004;49:389–410.
8. A.K. Gupta, D.J. Lloyd, Court SA. Precipitation hardening processes in an Al–0.4%Mg–1.3%Si–0.25%Fe aluminum alloy. Mater Sci Eng A 2001;301:140–6.
9. C.S. Tsao, C.Y. Chen, U.S. Jeng, T.Y. Kuo., Precipitation kinetics and transformation of metastable phases in Al–Mg–Si alloys. Acta Mater 2006;54:4621–31.
10. S. Esmaeili, S.X. Wang, D.J. Lloyd, W.J. Poole., On the precipitation-hardening behavior of the Al–Mg–Si–Cu alloy AA6111. Metall Mater Trans A 2003;34A:751–63
11. L.P. Troeger, E.A. Starke, "Microstructural and Mechanical Characterization of a Superplastic 6xxx Aluminum Alloy", Materials Science and Engineering, A277, 102-113, 2000.
12. G. J. Marshall, "Microstructural Control during Process-ing of Aluminium Canning Alloys," Journal of Materials Science, 1996, pp. 217-222.
13. S. Jiang, R. Wang., Grain size-dependent Mg/Si ratio effect on the microstructure and mechanical/electrical properties of Al-Mg-Si-Sc alloys, J. Mater. Sci. Technol. 35 (2019) 1354–1363
14. S.M. Hirth, G.J. Marshall, S.A. Court, D.J. Lloyd., "Effects of Si on the Aging Behaviour and Formability of Aluminium Alloys Based on AA6016", Materials Science and Engineering, A319- 321, 452-456, 2001.
15. E. Tan, B. Ögel., Influence of Heat Treatment on the Mechanical Properties of AA 6066, Alloy, Turkish J. Eng. Env. Sci. 31 (2007), pp. 53 – 60.
16. N. Anjabin and A. Karimi Taheri, The effect of aging treatment on mechanical properties of AA6082 alloy: modeling and experiment, Iranian Journal of Materials Science & Engineering Vol. 7, Number 2, Spring 2010
17. B. Milkereit et al, Continuous cooling precipitation diagrams of Al–Mg–Si alloys, Materials Science and Engineering A550 (2012) 87-96
18. M. Das, G. Das, M. Ghosh, M. Wegner, V. Rajnikant, S. G. Chowdhury, T.K. Pal., Microstructures and mechanical properties of HPT processed 6063 Al alloy, Materials Science & Engineering A 558 (2012) 525–532
19. J. Lan, X. Shen, J. Liu and L., Hua, Strengthening Mechanisms of 2A14 Aluminum Alloy with Cold Deformation Prior to Artificial Aging, Materials Science & Engineering A.
20. E. Tan and B. Ögel, "Influence of Heat Treatment on the Mechanical Properties AA6066 Alloy," *Turkish Journal of Engineering and Environmental Sciences*, Vol. 31, 2007, pp 53-60.
21. G. Al-Marahleh, "Effect of Heat Treatment Parameters on Distribution and Volume Fraction of Mg2Si in the Struc-tural Al 6063 Alloy," *American Journal of Applied Sci-ences*, Vol. 3, No. 5, 2006, pp. 1819-1823.
22. B. Milkereita, N. Wanderkab, C. Schickc, O. Kesslera., Continuous cooling precipitation diagrams of Al–Mg–Si alloys, Materials Science and Engineering A 550 (2012) 87– 96

AUTHOR PROFILE

Dr. Víctor Alcántara A., working as a professor in Mechanical Engineer Deparment of the National University of Trujillo-Peru. Mechanical engineer, Master in Materials Engineering (1996) and Doctor in Materials Science (2006) Lima-Peru. Member of the Materials Research Institute of the Post Graduate School at the National University of Trujillo. Specialization in characterization of ferrous and non-ferrous materials, carried out at the University of Cartagena of Spain. Author of multiple manuals and texts on materials and manufacturing processes. International speaker at multiple conferences in the Latin American region. Author of several articles in indexed journals